Monte Carlo Simulation of Size-Enlargement Mechanisms in Crystallization

John R. van Peborgh Gooch and Michael J. Hounslow
Dept. of Chemical Engineering, University of Cambridge, Cambridge CB2 3RA, U.K.

This article outlines a Monte Carlo approach for simulating crystallization processes both as an alternative to solving the population balance equations (PBE) and as a way of conducting multicoordinate simulations that are too complex to be solved as PBEs. First, simple cases with different combinations of nucleation, growth and aggregation are simulated for batch and continuous systems. The comparison of the results of these test cases with analytical and numerical results shows excellent agreement. New results for two cases with simultaneous growth rate dispersion and aggregation are also discussed. From these results, a new hypothesis is proposed to explain the observed reduction in the degree of aggregation for larger crystals in the continuous crystallization of potassium sulfate. The simulations show that this experimental observation may be caused by small, slow-growing crystals being swallowed by larger, fast-growing ones.

Introduction

The chemical engineer often uses energy and mass balances to describe and model the active mechanisms in chemical processes. In particulate processes, a number balance is also required to describe the number of particles and their important properties, such as size and shape. This number balance is formally referred to as the population balance (PB), and first appeared in the chemical engineering literature with the publication of work carried out by Hulburt and Katz (1964).

The PB is essentially a statement of continuity for a particulate population. In the PB, particulate properties are represented by a set of internal and external coordinates. External coordinates refer to the spatial location of a particle, and internal coordinates refer to properties of a particle, such as size. The PB has few physically meaningful analytical solutions, and usually requires numerical solution when describing the more complicated processes often observed in crystallization. The Monte Carlo approach is an alternative to posing and solving the PB.

Spielman and Levenspiel (1965) were the first to apply the Monte Carlo simulation method to particulate processes in order to study the influence of coalescence on reactions in the dispersed phase of two-phase systems in backmixed reactors. Others, notably Shah et al. (1977) and Ramkrishna (1981), developed a general simulation for particulate processes and established the precise mathematical connection between population balances and the Monte Carlo approach.

Monte Carlo methods have been applied to many particulate systems, especially biological populations, where the simulation of a large number of internal coordinates is desirable. However, the Monte Carlo simulation of a crystal population has not been done before, although Sengupta and Dutta (1991) looked at growth rate dispersion in a mixed suspension, mixed product removal (MSMPR) crystallizer, by simulating individual crystals. Other work has covered crystallization mechanisms, but from a more general, particulate process perspective; for example, Wright and Ramkrishna (1992) examined the self-perseving particle-size distribution (PSD) in aggregating batch systems.

We outline the Monte Carlo approach that we use to simulate crystallization processes. To test the simulations, one and two internal coordinate examples are given, describing batch and continuous systems. The Monte Carlo solutions are shown to agree well with existing numerical and analytical solutions to the PB. Then, three internal coordinates are used—size, growth rate and number of crystallites—to examine a crystallization system for which no analytical or numerical solution has yet been found. This system is simultaneous growth rate dispersion and aggregation in a batch crystallizer, and new simulation results are presented concerning how the PSD changes with time.

Correspondence concerning this article should be addressed to M. J. Hounslow.

A fourth internal coordinate—the swallowed crystallites coordinate—is added to model the number of small, slower-growing crystallites in an aggregate that are likely to lose their identity. Simulation results are presented of the product PSD of an MSMPR crystallizer in which simultaneous nucleation, growth rate dispersion, and aggregation occur. We use these new results to propose, and examine, an explanation for the observed reduction in the degree of aggregation for larger crystals in the continuous crystallization of potassium sulfate, as reported by Budz et al. (1987). This case also serves to show how the Monte Carlo technique can be used to conduct multicoordinate simulations that are too complex to be solved as population balance equations (PBE).

Crystallization and the Population Balance

In its most general form, the PB is expressed in terms of a set of external and internal coordinates of a particle, the vector $\boldsymbol{x}$, spanning the region over which the balance is performed. For a point in space this gives,

$$\frac{\partial n(\boldsymbol{x})}{\partial t} + \nabla\cdot[\boldsymbol{v}n(\boldsymbol{x})] - B(\boldsymbol{x}) + D(\boldsymbol{x}) = 0 \qquad (1)$$

where $B(\boldsymbol{x})$ and $D(\boldsymbol{x})$ are the birth and death terms respectively, $\boldsymbol{v}$ is the vector phase-space velocity, and $n(\boldsymbol{x})$ is the population density function. This equation is particularly useful in studying crystallization processes, as expounded by Randolph and Larson (1988).

In crystallization, the most important internal coordinate is often the size L, some characteristic length of the crystal. In a perfectly mixed system, external coordinates can be omitted from the PB and, therefore, with size as the only internal coordinate, Eq. 1 simplifies to

$$\frac{\partial n(L)}{\partial t} + \frac{d}{dL}[Gn(L)] - B(L) + D(L) = 0 \qquad (2)$$

where G is the crystal growth rate ($= dL/dt$). The population density $n(L)$ can now be directly related to the crystal size distribution (CSD), and for many simple processes, Eq. 2 can be solved analytically or numerically. Numerical solution of the PB is possible by recasting the problem in terms of a discretized population balance (DPB). However, for systems in which the CSD is affected by many factors, this becomes increasingly arduous. Such complex processes lend themselves to study by Monte Carlo simulation, the intrinsic simplicity of which allows the inclusion of several mechanisms and several internal coordinates in the problem.

Crystallization and Monte Carlo Simulation

The term Monte Carlo was first coined by Metropolis in 1947, and was used in the title of an article on diffusion of neutrons in fissionable material by Metropolis and Ulam (1949). The term is used to describe any approach to a problem where a probabilistic analog to a given mathematical problem is set up and solved by a stochastic sampling experiment. This invariably involves the generation of many random numbers, so giving rise to the name.

Following the pioneering work of Spielman and Levenspiel (1965) and Zeitlin and Tavlarides (1972) in applying the Monte Carlo technique to liquid-liquid dispersions, it is perhaps surprising that its application to crystallization processes is not widespread. It is only relatively recently that Sengupta and Dutta (1991) looked at growth rate dispersion in an MSMPR, with crystal shape and growth rate as the internal coordinates. However, in their work they did not simulate a crystal population, but simply simulated one crystal at a time. This elegant approach allowed them to build up a picture of the PSD of an exit stream from an MSMPR by giving each simulated crystal a residence time, randomly selected from the residence time distribution.

In contrast, the approach taken in this study has been to set up a crystal population within a rectangular array with each row representing one crystal, and each column an internal coordinate of that crystal. The variation of the population with time is simulated over a large number of small, discrete time steps. During each time interval, a series of array manipulations is performed to simulate the effect of the three mechanisms studied in this article, namely, nucleation, growth, and aggregation.

Shah et al. (1977) outlined a general approach for simulating particulate systems and introduced the concept of the interval of quiescence (IQ), or waiting time between particulate events. This allowed them to study small populations where it is likely that the random behavior of a single particle will lead to the random behavior of the entire population. In crystallization, the actual number of particles in even a small crystallizer is very large—typically 10^8 for a 1-L lab-scale crystallizer—and for the processes examined in this article the IQ is not required. However, the IQ may be required for some aggregating systems in which gelation occurs if one crystal becomes large enough for it to effectively aggregate with all other crystals in the crystallizer. This phenomenon occurs with some size-dependent aggregation kernels, and is discussed by Smit et al. (1994).

The mechanisms and the basic array manipulations that are required to simulate them are described. How the Monte Carlo simulation of batch processes can be simply extended to MSMPR simulation is explained and the simulation algorithms used for both is outlined. The simulations outlined in this article can be applied using a personal computer running the widely-used *Microsoft Excel* spreadsheet package with the array represented on a worksheet, and the code written in *Visual Basic*.

Nucleation

Nucleation is the term used to describe the formation of near-zero-size particles in a system—crystal birth. In this article, nuclei are taken to have zero-size, and so the birth rate is the product of the nucleation rate B_0 and the Dirac delta-function $\delta(L)$.

To simulate nucleation, new rows are added to the array. Each time a row is added, the values of the internal coordinates must be set. A coordinate might be some constant, e.g., the size will always equal zero, or a randomly generated property chosen from some predetermined distribution. An

example of the latter might be the growth rate g distributed according to the normalized distribution function $f_G(g)$, with a cumulative distribution function $F_G(g)$ given by

$$f_G(g) = \frac{1}{N}\frac{dN}{dg}$$

$$F_G(g) = \int_0^g f_G(g)dg \tag{3}$$

where N is the number of crystals. Then the growth rate for the jth crystal g_j can be generated from

$$g_j = F_G^{-1}(RND_j) \tag{4}$$

where RND_j is a random number between 0 and 1.

Growth

Growth is the term used to describe the enlargement of crystals by the gradual incorporation of ions, atoms or molecules into the crystal lattice. In this article, three common forms of the growth mechanism are taken:

Size-Independent Growth (SIG). The growth rate is constant (McCabe's ΔL law, first reported by McCabe (1929));

Size-Dependent Growth (SDG). The growth rate is some function of crystal size, invariably such that larger crystals grow faster; and

Growth Rate Dispersion (GRD). The growth rate is constant for any one crystal, but different for each crystal, resulting in a distribution of growth rates.

To simulate crystal growth over a given time, the new size is simply calculated from the particle's current size, and growth rate. Hence for a time interval Δt

$$L_{new} = L_{old} + G\Delta t \tag{5}$$

where G can be a function of the crystal coordinates. The form of this relationship between G and the internal coordinates is given, as necessary, with the case studies.

Aggregation

We use aggregation to describe any combination of two particles to form one larger particle. In this article, only size-independent aggregation is considered, for which the rate of change of m_0, the total number of crystals per unit volume, due to aggregation, is given by,

$$\frac{dm_0}{dt} = -\frac{1}{2}\beta_0 m_0^2 \tag{6}$$

where β_0 is the aggregation rate constant. When describing aggregation processes, it is convenient to express the extent of aggregation quantitatively, and in this article we use the index of aggregation I_{agg} defined by Hounslow (1990) as

$$I_{agg} = \begin{cases} 1 - \dfrac{m_0}{m_0^{in}} & \text{continuous crystallizer} \\ 1 - \dfrac{m_0}{m_0^{\phi}} & \text{batch crystallizer} \end{cases} \tag{7}$$

where m_0^{in} and m_0^{ϕ} are the total number of crystals in the feed and charge respectively. In continuous systems, m_0^{in} also includes nucleated crystals.

Just as the incorporation of aggregation into the PB requires a death term and a birth term, so it does with Monte Carlo simulation. First, the two crystals that will form the aggregate must be selected at random, and removed from the array. Then a new row is added to represent the aggregated crystal with coordinates calculated as a function of the coordinates of the two aggregating crystals. For example, when two crystals aggregate, volume is conserved, and we can relate the size L_{agg} of the resulting aggregate to the sizes L_{a1} and L_{a2} of the two aggregating crystals by

$$L_{agg} = (L_{a2}^3 + L_{a1}^3)^{1/3} \tag{8}$$

Other relationships for calculating the internal coordinates of the aggregate are given later, as necessary, with the appropriate case studies.

Batch simulation

In this article, we report simulation results for batch crystallization with constant supersaturation, and no nucleation. To perform these simulations, the program MCB was written, an outline of which is shown in Figure 1. The crystal population is represented in an array with N_c rows, to represent the crystals, and N_i columns, for the internal coordinates. The shorthand $X_{j,k}$ is used to refer to the kth internal coordinate of the jth crystal (row j, column k in the array). N_c is only a tiny fraction of m_0, the real number of crystals per unit volume, and in this work m_0/N_c is of the order 10^7.

To represent the charge of the vessel, each row in the array is initialized in a similar way to the nucleation simulation described above. For example, to produce a charge PSD that is distributed according to the normalized distribution function $f_L(L)$, the size of the jth crystal, L_j is generated from

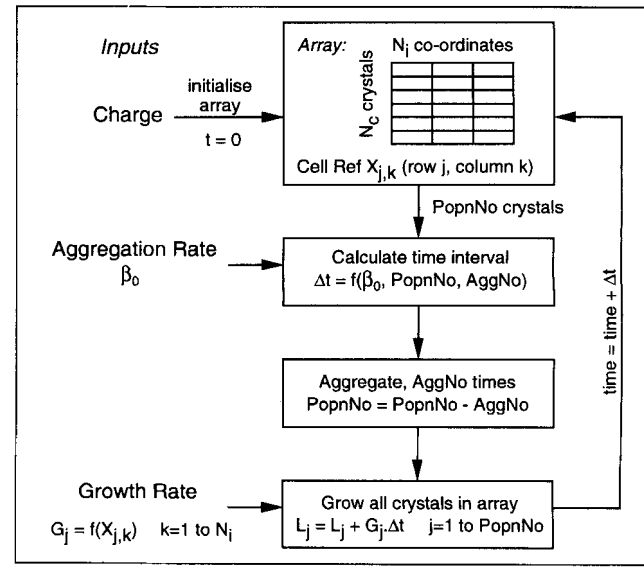

Figure 1. MCB program: Monte Carlo batch.

$$L_j = F_L^{-1}(RND_j) \quad \text{for} \quad j = 1 \text{ to } N_c \tag{9}$$

where $F_L(L)$ is the cumulative distribution.

With the array initialized, the program then simulates the effect of the mechanisms on the crystal population in a series of time steps of variable duration Δt. For convenience, this time interval is calculated from the aggregation rate, so that there is an integer number of aggregation events per time interval. Integrating Eq. 6 gives

$$\Delta t = \frac{2\Delta m_0}{\beta_0 m_0 (m_0 - \Delta m_0)} \tag{10}$$

where Δm_0 is the change in m_0 due to aggregation. Having calculated Δt, *AggNo* aggregation events are performed, where

$$AggNo = \frac{PopnNo\,\Delta m_0}{m_0} \tag{11}$$

PopnNo in this equation is the number of simulated crystals, initially equal to N_c.

After aggregation, growth is simulated, although if more convenient this order can be reversed with no effect on the accuracy. Every crystal is grown, with the new size of the jth crystal calculated using Eq. 5, where G is some function of the internal coordinates $f(X_{j,1} \ldots X_{j,k})$ dependent on the growth mechanism chosen. After the growth step, a new Δt is calculated and the process repeated.

By choosing a small value for *AggNo*, and hence a small time interval, the error caused by the discretization of time is reduced. In particular, when simulating simultaneous growth and aggregation, a small *AggNo* such as 5 reduces the error created by simulating the mechanisms in series, rather than in parallel. In the limit *AggNo* can be 1, although the improvement in simulation accuracy is counterbalanced by a decrease in speed.

As and when desired, the array contents are stored, so that a picture is built up of how the properties of the population change with time. The results are often best presented in some form of histogram by binning data by size, for example, and calculating the average value of some other coordinate for each size interval. The accuracy of the results is improved by having either a larger number of rows in the array, or by increasing the number of times the simulation is run.

MSMPR simulation

In this article, we report simulation results for the steady-state operation of an MSMPR crystallizer with no feed. To perform these simulations, the program MCM was written, an outline of which is shown in Figure 2. Many of the components of MCM are the same as those in MCB with the crystal population represented by an array, and each mechanism simulated in turn during a time interval Δt.

At steady state, none of the active mechanisms is time-dependent, and, for the population as a whole, the properties are not time variant, and therefore, unlike MCB, the time interval Δt can be constant. The aggregation and growth mechanisms are applied in the same way as in the batch program, and indeed share the same subroutines. In addition to these mechanisms, the outlet stream and nucleation mechanism are also simulated.

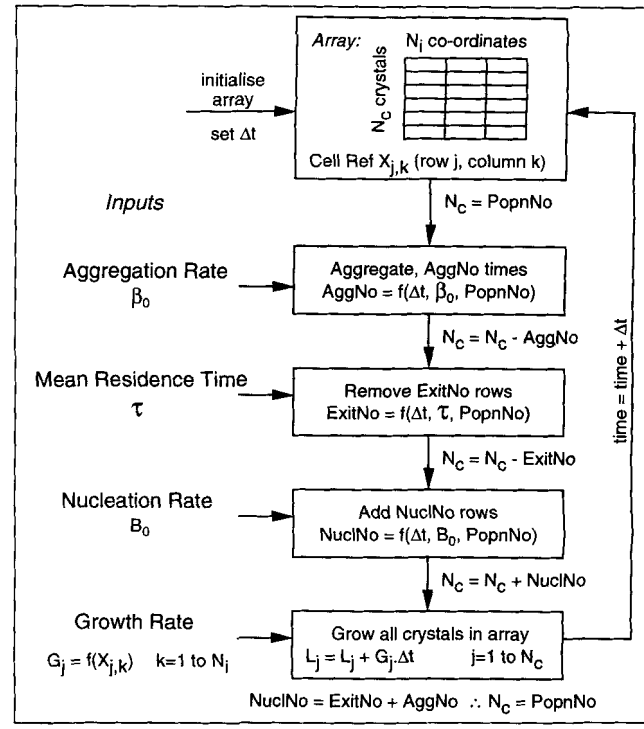

Figure 2. MCM program: Monte Carlo MSMPR.

To simulate an output stream, rows are simply removed from the array at a rate governed by the mean residence time τ. In the program, the number of rows to be removed is called *ExitNo*, and must be an integer value calculated from the equation

$$ExitNo = \frac{PopnNo\,\Delta t}{\tau} \tag{12}$$

where *PopnNo* is taken to be constant.

To simulate nucleation, new rows are simply added to the array at a rate governed by the nucleation rate. In the program, the number of rows to be added is called *NuclNo*, and again must be an integer value calculated from the equation

$$NuclNo = \frac{B_0\,\Delta t\,PopnNo}{m_0} \tag{13}$$

At steady state, the net effect of these three actions must be to leave the number of rows unchanged, and therefore not all combinations of β_0, τ, B_0 and N_c can be chosen.

The array can be initialized with a random charge, as virtually all the original crystals will be washed out during the time the simulation is left to reach steady state. This time is typically 10–15 mean residence times, after which mean properties of the distribution, like crystal size, are virtually constant. Steady state is achieved because the random removal of crystals, governed by Eq. 12, accurately reproduces the residence time distribution for an MSMPR crystallizer. Having reached steady state, samples can be taken intermit-

tently by storing the entire array, not just the outlet stream, so the number of crystals in each sample and therefore the accuracy increases.

One Internal Coordinate Problem

In this section we examine two test cases for which the PB has known analytical solutions, and for which only one internal coordinate is necessary. These two simple problems are used to assess the accuracy of the Monte Carlo simulation method in batch and continuous systems.

Case study 1: aggregation only in a batch crystallizer

In this analysis, length is the only internal coordinate to be examined. Also, only one mechanism is considered, aggregation, and Eq. 2 reduces to:

$$\frac{\partial n(L)}{\partial t} = B(L) - D(L) \tag{14}$$

For size-independent aggregation, Gelbard and Seinfeld (1978) have shown that when the charge of the batch vessel is given by

$$n(L) = \frac{N_0 z^2}{L_0} \exp(-z^3) \tag{15}$$

then the product PSD is

$$n(L) = \frac{4N_0 z^2}{L_0(Y+2)^2} \exp\left(-\frac{2z^3}{(Y+2)}\right) \tag{16}$$

where N_0 is the initial number of crystals, z is L/L_0, L_0 is the cube root of the mean volume of the charge, and $Y = N_0 \beta_0 t$. This analytical result is referred to as the self-preserving PSD, as the form of the distribution does not vary with time.

The array is initialized with the size internal coordinate calculated using Eq. 9 to produce the required size distribution, given in Eq. 15. The effect of aggregation on the array is simply to reduce the number of rows. The only coordinate equation is that for the size of a new aggregate as shown in Eq. 8.

The Monte Carlo simulation results are compared with the analytical solution in Figure 3 for an I_{agg} of 0.875. To simulate such a high index of aggregation, it is necessary to have a very large initial number of crystals to avoid the population becoming too small to be statistically representative. This large number can be achieved in two ways: by running MCB once with a very large initial array, or by combining the results of several runs each with a smaller array. The choice is based on which method is the quickest, as provided the total numbers are the same the error will be no different in each case. In this case, MCB was run with an initial population of 25,600 to produce a final population of 3,200.

The simulation results agree very well with the analytical solutions, with most scatter observed at each end of the simulated product PSD. This is due to the smaller number of crystals at the two tails of the distribution, resulting in a larger percentage error, as indicated by the error bars, which show the 95% confidence limits for each point.

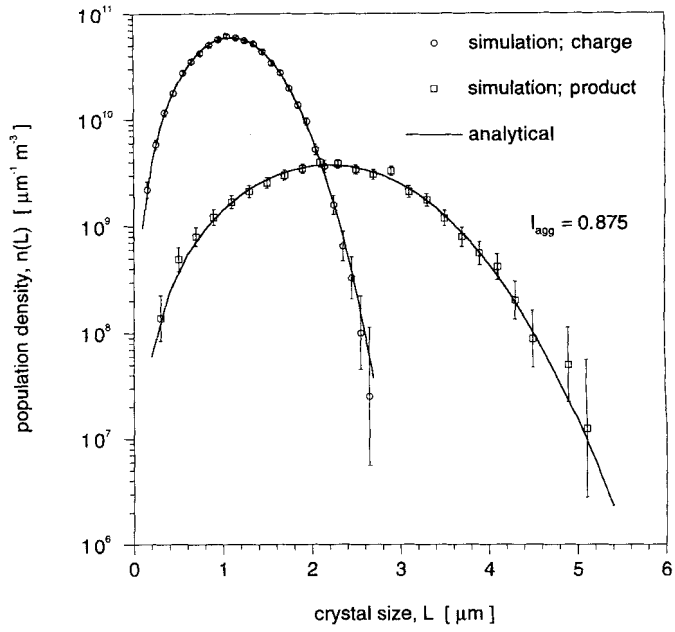

Figure 3. Self-preserving PSD in a batch crystallizer with aggregation only.

Case study 2: nucleation and size-dependent growth in an MSMPR crystallizer

Two mechanisms, nucleation and growth, are simulated in an MSMPR crystallizer, with length as the only internal coordinate. For this system, the form of the PB given in Eq. 2 simplifies to

$$\frac{\partial[G(L)n(L)]}{\partial L} + \frac{n(L)}{\tau} = B_0 \delta(L) \tag{17}$$

There is no need to add the growth rate as another internal coordinate because, in this case, the growth rate is dependent on size. There have been many proposed forms for size-dependent growth, and in this article we use perhaps the most popular and widely recognized relationship, the ASL equation, first published by Abegg et al. (1968)

$$G(L) = G_0(1+\gamma L)^b \qquad b > 1 \tag{18}$$

With this growth rate function, Eq. 17 can be solved analytically to give

$$n(L) = \frac{B_0}{G_0}(1+\gamma L)^{-b} \exp\left(\frac{1-(1+\gamma L)^{1-b}}{G_0 \tau \gamma (1-b)}\right) \tag{19}$$

To simulate this, the growth rate at each time step is calculated from the approximation, valid for small Δt, that

$$L_{new} = L_{old} + \Delta t G_0 (1+\gamma L_{old})^b \tag{20}$$

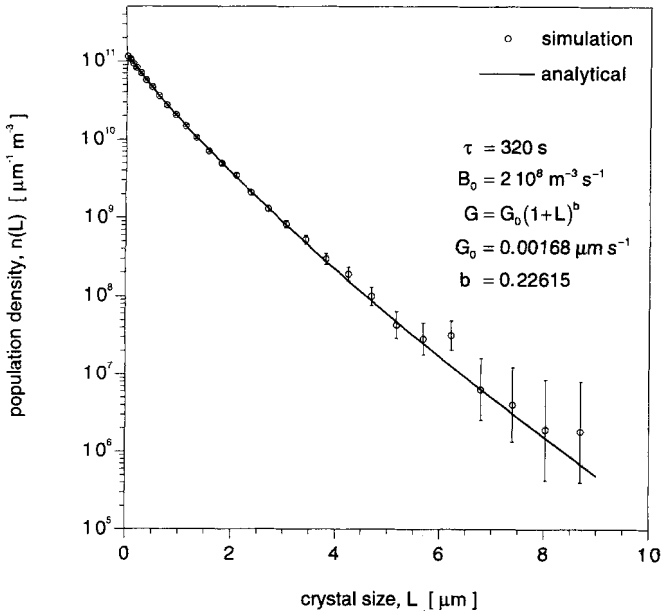

Figure 4. Nucleation and size-dependent growth in an MSMPR crystallizer.

In this case study, $\gamma = 1\ \mu m^{-1}$, and $b = 0.22615$. To simulate nucleation, a new row is added with the size coordinate set equal to zero.

The number of rows in the array was 6,400, and just 8 samples were taken, with 500 s simulated time in between, giving a total sample size of 51,200. The simulation results are compared to the analytical solution in Figure 4, and again found to be in good agreement with more scatter at lower population density as expected. The error bars again show the 95% confidence limits for each point. The scatter in the data can be reduced dramatically by taking more samples, however, the scatter shown in this figure is entirely comparable with the most accurate experimental measurements.

In this case, as with all the examples in this article, growth rates of the order of 0.002 $\mu m\ s^{-1}$ and mean residence times of the order of several minutes are used. The results however can be used for other combinations of growth rate and τ, with the only effect being to scale the size axis in proportion to $G\tau$.

Two Internal Coordinate Problems

Having tested the accuracy of the simulations with simple cases which have analytical solutions, in this section we can now test the simulations with more complicated problems that require numerical solution. We compare the Monte Carlo results to solutions obtained using a DPB, the Lister et al. (1995) extension of the DPB of Hounslow et al. (1988), that allows simultaneous nucleation, growth and aggregation.

Case study 3: growth rate dispersion in a batch crystallizer

To represent growth rate dispersion (GRD) mathematically, a two-dimensional population density function $f_g(L, g)$, can be defined as

$$n(L) = \int_0^\infty f_g(L, g)\, dg \tag{21}$$

Now there are two internal coordinates, size and growth rate. For growth rate dispersion in a batch system, Eq. 1 becomes

$$\frac{\partial f_g(L,g)}{\partial t} + \frac{\partial}{\partial L}(g f_g(L,g)) = 0 \tag{22}$$

with the initial condition $f_g(L, g)$ at $t = 0$ is $f_{in}(L, g)$.

In this case, the normalized distribution of growth rates $f_G(g)$ is assumed to be the same for all L in the charge. With this simplification the PSD after a time t is given by

$$n(L) = \frac{1}{t}\int_0^L n_{in}(l) f_G\left(\frac{L-l}{t}\right) dl \tag{23}$$

where the charge is represented by the population density $n_{in}(l)$. Although Eq. 23 is an analytical expression, it requires numerical solution, which was performed using the *Mathematica* package.

The Monte Carlo simulation was carried out as in the first case study, but now with two columns in the array for size and growth rate and with only 6,400 rows. The log-normal distribution was used to generate the size coordinates of the charge, using Eq. 9 with a mean size of 2 μm and a standard deviation of 1.3 μm. The inverse-gamma distribution of Janse and de Jong (1978) was used to generate the growth rate coordinates in a similar way, where $f_G(g)$ is given by

$$f_G(g) = \frac{a^{(K-1)}}{\Gamma(K-1)} g^{-K} \exp\left(-\frac{a}{g}\right) \tag{24}$$

with $a = 0.01$ and $K = 7$, giving a mean of 0.002 $\mu m\ s^{-1}$, and a standard deviation of 0.001 $\mu m\ s^{-1}$.

The numerical results from Eq. 23 are compared to the Monte Carlo simulation results in Figure 5, and are seen to be in good agreement. In the case shown, the simulation results are based on 3 runs, giving a total sample size of 19,200.

With two internal coordinates, we can also look at how one coordinate is correlated to another. From the result in Eq. 21, we can develop an expression for the population-mean growth rate of crystals $\bar{g}(L)$ as

$$\bar{g}(L) = \frac{1}{t^2 n(L)}\left[\int_0^L n_{in}(l) f_G\left(\frac{L-l}{t}\right)(L-l)\, dl\right] \tag{25}$$

This numerical result is compared to the simulation results in Figure 6, and again the simulation and numerical results are in close agreement. This result also clearly demonstrates how GRD can result in the apparent size-dependence of the growth rate.

Case study 4: nucleation, growth and aggregation in an MSMPR crystallizer

When two single crystals aggregate, the resulting crystal can be thought of as one crystal containing two crystallites. By extension, the number of crystallites per crystal c can be

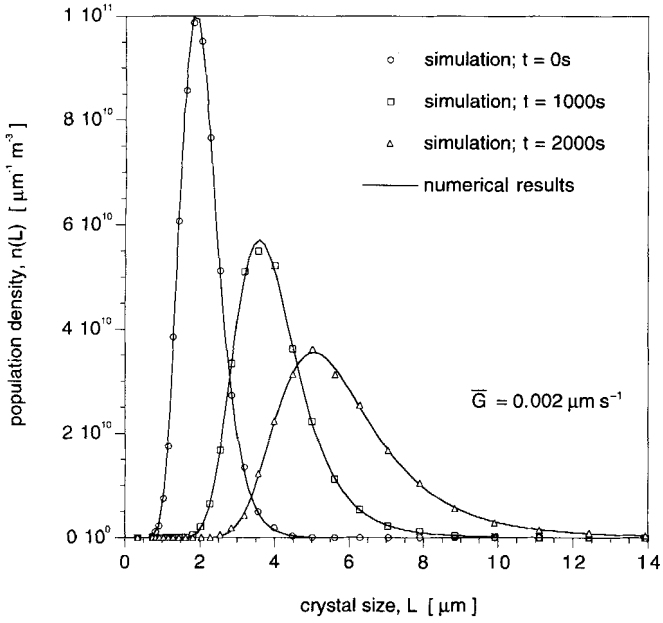

Figure 5. Growth rate dispersion in a batch crystallizer.

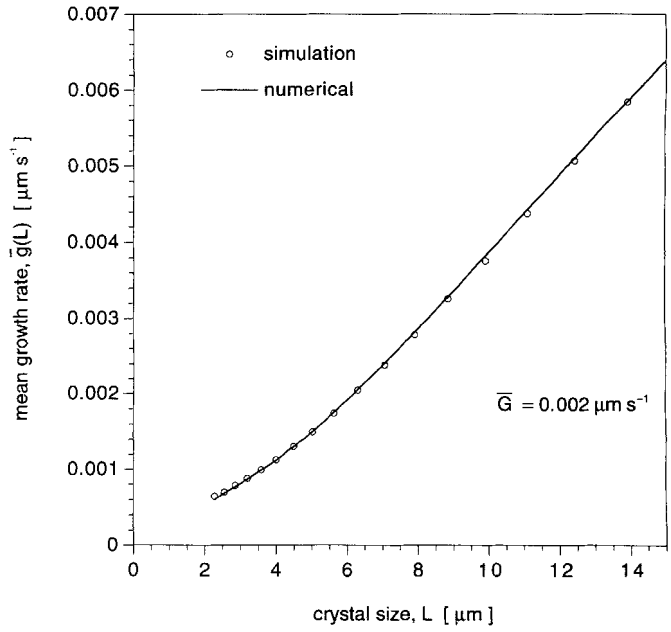

Figure 6. Mean growth rate against size for growth rate dispersion in a batch crystallizer.

thought of as an internal coordinate. In this case study, the two coordinates chosen are L and c, and the number density is related to the two-dimensional population density function $f_c(L,c)$ by

$$n(L) = \int_0^\infty f_c(L,c)dc \tag{26}$$

The PB for an MSMPR crystallizer, with nucleation, size-independent growth and aggregation, can then be written as

$$\frac{\partial}{\partial L}[Gf(L,c)] + \frac{\partial}{\partial c}\left(\frac{dc}{dt}f(L,c)\right) = B(L,c) - D(L,c) \tag{27}$$

Currently, there is no analytical solution to this equation, even with size as the only internal coordinate. However, it can be shown that the population density of single crystals, $n_1(L)$, is given by

$$n_1(L) = \frac{B^0}{G}\exp\left[-\frac{L}{G}\left(\frac{1}{\tau} + \beta_0 m_0\right)\right] \tag{28}$$

Also a DPB can be used to solve the PB numerically for simultaneous nucleation, growth and aggregation with length as the only internal coordinate.

To simulate this process, the approach taken in the second case study is extended and relationships developed for the new internal coordinate c. This is reasonably trivial: for nuclei, $c = 1$, growth has no effect on c, and the relationship for aggregation is simply

$$c_{agg} = c_{a1} + c_{a2} \tag{29}$$

The array was again set up with 6,400 rows, but the number of samples was expanded from 8 to 100. The simulation results are compared to the analytical result for single crystals given above, and the numerical solution from a DPB, in Figure 7, for an $I_{agg} = 0.167$ and a growth rate of 0.002 μm·s^{-1}. The results are in very good agreement, with the increase in sample size to 640,000 resulting in considerably less scatter in the Monte Carlo simulation results.

We can now also use the second internal coordinate c to plot the degree of aggregation P defined by Budz et al. (1987) as

$$P_i = \left[\frac{N_{agg}}{N_{agg} + N_{dc}}\right]_i \tag{30}$$

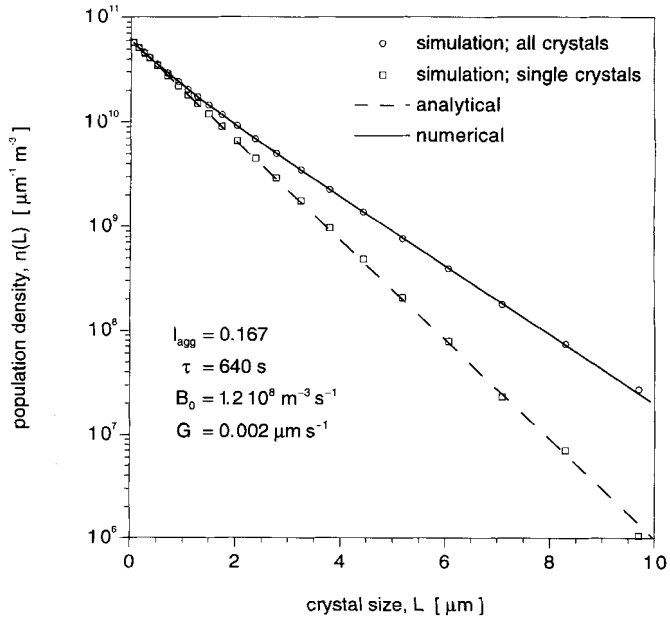

Figure 7. Nucleation, size-independent growth and aggregation in an MSMPR crystallizer.

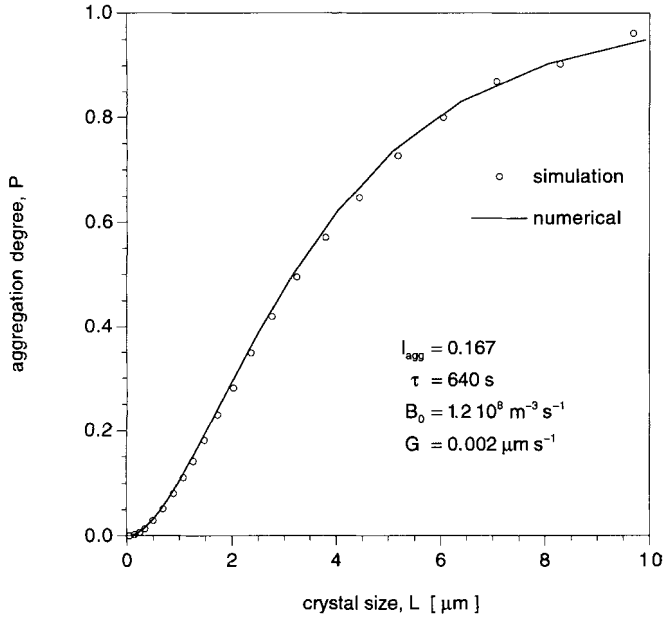

Figure 8. Degree of aggregation for nucleation, size-independent growth and aggregation in an MSMPR crystallizer.

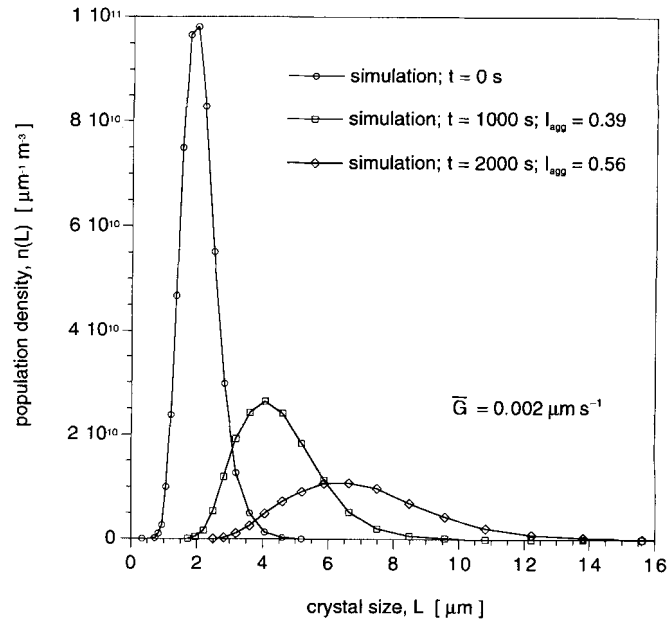

Figure 9. Growth rate dispersion and aggregation in a batch crystallizer.

where i is the size interval, N_{agg} is the number of aggregates, and N_{dc} is the number of discrete crystals (single crystals). These results are shown in Figure 8, where we can see that the degree of aggregation increases monotonically with size. This is as expected—the longer a particle remains in the crystallizer, the larger it gets, and the higher the chance that it will aggregate. We also show the degree of aggregation calculated from the analytical result in Eq. 28, and the DPB.

Three Internal Coordinate Problems

In the first two sections we have shown that the Monte Carlo technique can accurately simulate the PSD. In the cases given so far, the technique offers few advantages over other solution methods. In particular, the computational inefficiency of Monte Carlo simulation will often make a DPB or other such techniques preferable when there is a choice. However, in this section we look at a system which is too complex to be solved as a PBE. We report the results of simulations which allow us to study for the first time some of the more complex interactions that exist in crystallization processes, and three crystal properties.

Case study 5: growth rate dispersion, and aggregation in a batch crystallizer

In this case study, we use all the internal coordinates used thus far—size, growth rate, and number of crystallites. The Monte Carlo simulation approach is the only way in which such a problem can be tackled simply. The reason why existing DPBs cannot produce a numerical solution is that we now must consider what the growth rate of a new aggregate is when the two particles that combine are growing at different rates.

To tackle this problem in Monte Carlo simulations, a mathematical relationship between the growth rate of an aggregate and the internal coordinates of the two aggregating crystals must be developed. It seems reasonable to take some average of the two growth rates, as there is no reason to assume that a crystal will forget its intrinsic growth rate. It then seems logical to weight this average by the surface areas of the two aggregate precursors. Hence, in addition to Eq. 6 for L_{agg} and Eq. 29 for c_{agg}, we can calculate the growth rate g_{agg} of the aggregate from

$$g_{agg} = (L_{a1}^2 g_{a1} + L_{a2}^2 g_{a2})/(L_{a1}^2 + L_{a2}^2) \qquad (31)$$

The array is initialized in the same way as in the third case study, with the extra coordinate c set equal to 1. The same growth rate distribution function is used, and the same combination of 6,400 rows and three samples. In Figure 9 the simulation results are presented for an I_{agg} of 0.56. Compared to Figure 5, we see how the combination of GRD and aggregation results in exaggerated broadening and flattening of the PSD, as expected. In this article, there is unfortunately no space for a comparison of these simulation results with experimental data, although we hope to explore this issue in a future article.

Four Internal Coordinate Problems

In this section, we give an example of a four internal coordinate simulation to again study a system where more conventional techniques currently fail. We aim to show how the Monte Carlo simulation method can be used to analyze experimental results, and test a hypothesis to explain them.

Case study 6: nucleation, GRD and aggregation in an MSMPR crystallizer

The crystallization process in this case is the same as in the fourth case study, but this time there is also a distribution of

Table 1. Equations for Crystallite and Swallowed Crystallite Internal Coordinates

Condition	Relation
If $L_{a1} > L_{a2}$ and $g_{a1} > 3g_{a2}$	$c_{agg} = c_{a1}$ $s_{agg} = s_{a1} + s_{a2} + c_{a2}$
If $L_{a2} > L_{a1}$ and $g_{a2} > 3g_{a1}$	$c_{agg} = c_{a2}$ $s_{agg} = s_{a1} + s_{a2} + c_{a1}$
All other cases	$c_{agg} = c_{a1} + c_{a2}$ $s_{agg} = s_{a1} + s_{a2}$

growth rates. Therefore, an extra internal coordinate for a crystal's intrinsic growth rate must be considered as well as size and the number of crystallites. The fourth internal coordinate is the swallowed crystallite coordinate s. This is used to count the number of small, slower-growing crystallites within an aggregate, which are consequently likely to lose their identity as the aggregate grows.

Only simulation of aggregation is complicated by the addition of s. Nucleation simulation is trivial with $L = 0$, g generated from Eq. 4, $c = 1$ and $s = 0$, and growth only affects L. With aggregation, the evaluation of c and s is conditional on the relative sizes and growth rates of the two aggregating crystals. The rule adopted was that if the larger particle had a growth rate three times the growth rate of the smaller particle, then the smaller crystal would be swallowed. This conditional mathematical relationship is given in Table 1.

In Figure 10, we show the results for the simulation of the population density of crystals for an $I_{agg} = 0.167$. These results were obtained using an array with 6,400 rows and taking 240 samples, at 128 s intervals. This results in a very smooth curve indeed, as can be seen, with the error bars again representing the 95% confidence limits. The time between samples is less than the mean residence time, but is sufficient for the crystals in any given bin to be almost completely replaced. Therefore, although every sample as a whole is correlated with the previous one, each estimate of the population density in a given bin is independent.

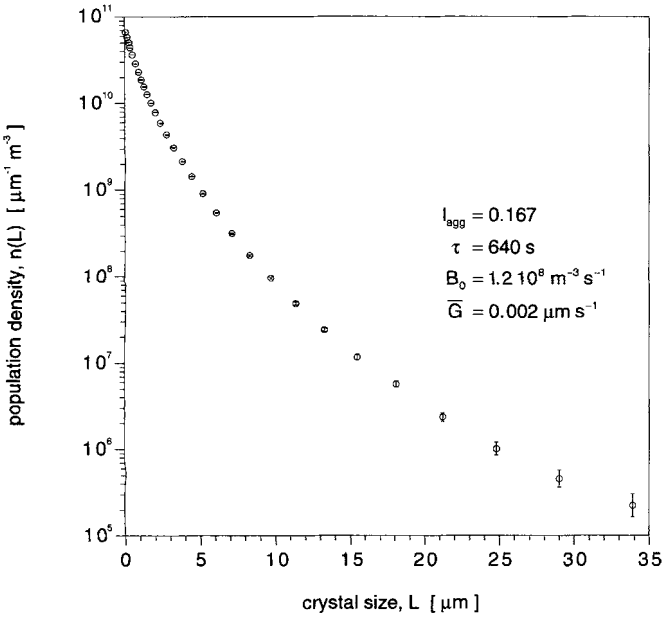

Figure 10. Nucleation, growth rate dispersion and aggregation in an MSMPR crystallizer.

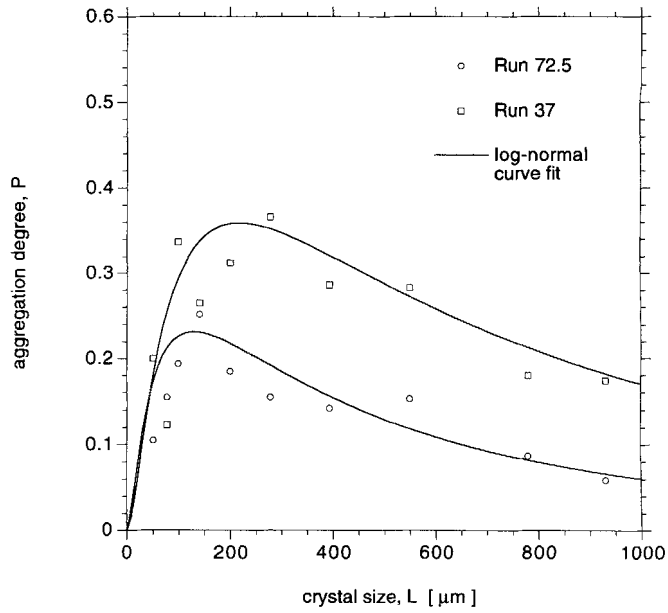

Figure 11. Degree of aggregation, (K_2SO_4 crystals) after Budz et al. (1987).

Comparison with experimental results

Figure 11 shows the results obtained by Budz et al. (1987) for the degree of aggregation in a potassium sulfate system in an MSMPR. Potassium sulfate has been studied widely in relation to the growth mechanism, for which many people have suggested that there is SDG or GRD, e.g., Jones and Mydlarz (1989).

Budz et al. describe the hump in the $P(L)$ curve as interesting, which is understandable when one considers the results of the Monte Carlo simulation result shown in Figure 8. One would think that the largest crystals would be aggregates, and that P should rise monotonically with L. Budz et al. suggest, as they say, tentatively, that this is caused by a combination of size-dependent aggregation and size-dependent breakage operating as competing mechanisms in the crystallizer, and that above some critical size, the breakage becomes dominant, and the degree of aggregation decreases.

In this section, we suggest an alternative explanation which does not necessitate the introduction of a size-dependent breakage mechanism. We propose that growth and aggregation can explain this observation, and have used the simulations to verify whether our hypothesis could lead to the observed maximum in the $P(L)$ curve.

In Figure 12 the average number of crystallites has been plotted against size. Two results are shown—one with all crystallites labeled "true," and another with only those crystallites that are likely to retain their identity within the aggregate labeled "apparent." The apparent average number of crystallites is seen to fall off with size. This is because the larger crystals in the system are likely to be those with the larger growth rates, and the crystals with the larger growth

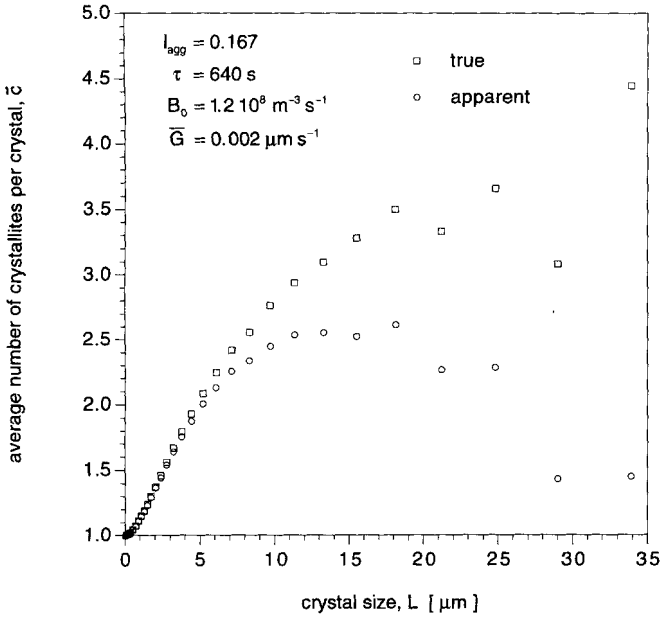

Figure 12. Average number of crystallites per crystal for nucleation, GRD and aggregation in an MSMPR crystallizer.

rates are more likely to swallow any smaller crystal with which they aggregate. Hence, the proportion of swallowed crystallites will be highest for the largest crystals.

In Figure 13, the effect of this phenomenon on the observed degree of aggregation is shown. We have made no effort to superimpose our simulation results on those of Budz et al., but the curve shown on the diagram has the same log-normal form as suggested by Budz et al. and seems to fit the data well. We have merely used the simulation results to test a hypothesis, and the data represented here are the first results achieved—no adjustment of parameters was necessary to get the observed hump. Having tested the hypothesis, more extensive simulation work could help to design a series of experiments to fully investigate the interaction between the two size-enlargement mechanisms, and provide a true test for the validity of the proposal. However, we do believe that this work shows how our Monte Carlo simulations can be used to test theories concerning the interaction between mechanisms that would be unexaminable by any other means.

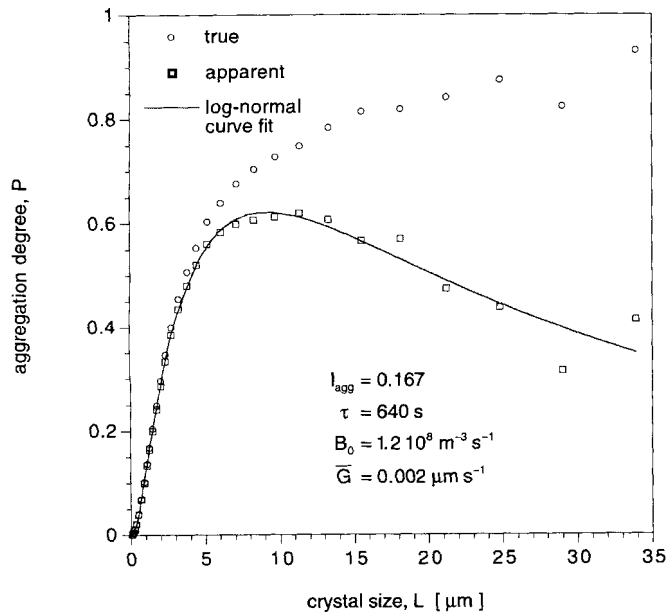

Figure 13. Degree of aggregation for nucleation, GRD and aggregation in an MSMPR crystallizer.

Hardware and Software

In this work, the main objective was to create a flexible, easy to use package, that would have the widest possible range of users. To this end, we have taken advantage of the ever increasing power of desktop machines, and the software they run: the combination of an Apple Power Macintosh 7100/80 with the standard spreadsheet package Microsoft Excel was chosen. Excel has the distinct advantage of being virtually identical on the Windows and the Macintosh platforms, and is also now bundled with the high-level programming language Visual Basic. This combination allows the user to analyze results quickly with all the graphical and statistical options available within the same package.

The time for simulations varied according to the complexity of the system, and the number of samples taken. In Table 2, we show the time taken for each of the simulations reported. The times for MSMPR simulations includes the time for the simulated population to equilibrate, as well as the time to take the samples.

Conclusion

We have outlined a simple Monte Carlo approach that can be used to simulate crystallization processes, or other particulate processes, on a desktop computer using common spreadsheet software. We have shown how simulation of batch processes can be extended to the simulation of continuous processes at steady state, and how an indefinite number of internal coordinates can be modeled. We have used test cases to check the validity of this approach, and then moved on to consider examples of systems that are too complex to be solved using conventional techniques.

Table 2. Computer Times for Monte Carlo Simulations

Case	System	N_c	Samples	Time
1	Batch Aggregation Only	25,600	1	3 min
2	MSMPR Nucleation and SDG	6,400	8	120 min
3	Batch GRD only	6,400	3	3 min
4	MSMPR Nucleation, Growth and Aggregation	6,400	100	320 min
5	Batch GRD and Aggregation	6,400	3	100 min
6	MSMPR Nucleation, GRD and Aggregation	6,400	250	620 min

In the final case we used the capabilities of this technique to examine how size-enlargement mechanisms interact. Four internal coordinates were used—size, growth rate, number of crystallites, and the swallowed crystallites coordinate. We presented simulation results for a continuous crystallizer in which simultaneous nucleation, growth rate dispersion, and aggregation occurs. From these results, a new hypothesis was proposed to explain the observed reduction in the degree of aggregation for larger crystals in the continuous crystallization of potassium sulfate. By using the Monte Carlo simulations, we have shown that this experimental observation may be caused by small, slow-growing crystals being swallowed by larger, fast-growing ones. This work shows how the optical analysis of a crystal product form cannot be relied on to quantify aggregation rates, when growth rate dispersion is active.

Acknowledgments

We would like to thank the Engineering and Physical Sciences Research Council and the Royal Academy of Engineering for their financial support. We would also like to thank Dr. Nigel Seaton for his expert advice on the presentation of the Monte Carlo simulation method and results. Finally, much thanks also to Ed Wynn for his magnificent help in the preparation of this article.

Literature Cited

Abegg, C. F., J. D. Stevens, and M. A. Larson, "Crystal Size Distributions in Continuous Crystallizers when Growth is Size Dependent," *AIChE J.*, **14**(1), 118 (1968).

Budz, J., A. G. Jones, and J. W. Mullin, "Agglomeration of Potassium Sulphate Crystals in MSMPR Crystallizer," *AIChE Symp. Ser.*, No. 253, **83**, 78 (1987).

Gelbard, F., and J. H. Seinfeld, "Numerical Solutions of the Dynamic Equation for Particulate Systems," *J. Comp. Phys.*, **28**, 357 (1978).

Hounslow, M. J., R. L. Ryall, and V. R. Marshall, "A Discretized Population Balance for Nucleation, Growth and Aggregation," *AIChE J.*, **34**(11), 1821 (1988).

Hounslow, M. J., "A Discretized Population Balance for Continuous Systems at Steady State," *AIChE J.*, **36**(1), 106 (1990).

Hulburt, H. M., and S. L. Katz, "Some Problems in Particle Technology: A Statistical Mechanical Formulation," *Chem. Eng. Sci.*, **19**, 555 (1964).

Janse, A. H., and E. J. de Jong, "The Occurrence of Growth Dispersion and its Consequences," *Industrial Crystallization*, p. 145, Plenum Press, New York (1978).

Jones, A. G., and J. Mydlarz, "Continuous Crystallization and Subsequent Solid-Liquid Separation of Potassium Sulphate Part 1: MSMPR Kinetics," *Chem. Eng. Res. Dev.*, **67**, 283 (1989).

Litster, J. D., D. J. Smit, and M. J. Hounslow, "Adjustable Discretized Population Balance for Growth and Aggregation," *AIChE J.*, **41**(3), 591 (1995).

McCabe, W. L., "Crystal Growth in Aqueous Solutions," *Ind. Eng. Chem.*, **21**(1), 30 (1929).

Metropolis, N., and Ulam, S., "The Monte Carlo Method," *J. Am. Stat. Ass.*, **44**, 335 (1949).

Ramkrishna, D., "Analysis of Population Balance—IV. The Precise Connection Between Monte Carlo Simulation and Population Balances," *Chem. Eng. Sci.*, **36**, 1203 (1981).

Randolph, A. D., and M. A. Larson, *Theory of Particulate Processes*, 2nd ed., Academic Press (1988).

Sengupta, B., and T. K. Dutta, "Monte-Carlo Simulation of the Crystal Size Distribution in a Continuous Sucrose Crystallizer," *Chem. Eng. J. and Biochem. Eng. J.*, **46**(2), B35 (1991).

Shah, B. H., J. D. Borwanker, and D. Ramkrishna, "Simulation of Particulate Systems Using the Concept of the Interval of Quiescence," *AIChE J.*, **23**, 897 (1977).

Smit, D. J., M. J. Hounslow, and W. R. Paterson, "Aggregation and Gelation: 1. Analytical Solutions for CST and Batch Operation," *Chem. Eng. Sci.*, **49**(7), 1025 (1994).

Spielman, L. A., and O. Levenspiel, "A Monte Carlo Treatment of Reacting and Coalescing Dispersed Phase Systems," *Chem. Eng. Sci.*, **20**, 247 (1965).

Wright, H., and D. Ramkrishna, "Solutions of Inverse Problems in Population Balances. 1. Aggregation Kinetics," *Comp. Chem. Eng.*, **16**(12), 1019 (1992).

Zeitlin, M. A., and L. L. Tavlarides J., "Fluid-Fluid Interactions and Hydrodynamics in Agitated Dispersions: A Simulation Model," *Can. J. Chem. Eng.*, **50**, 207 (1972).

Manuscript received Aug. 24, 1995, and revision received Oct. 24, 1995.